MINERALOGIA, *40, No. 1–4: 65–84 (2009)*
DOI: 10.2478/v10002-009-0003-2
www.Mineralogia.pl

MINERALOGICAL SOCIETY OF POLAND
POLSKIE TOWARZYSTWO MINERALOGICZNE

Original paper

Mineralization of teeth and bones of the cave bear (*Ursus spelaeus*) from the Biśnik Cave, Southern Poland

Anna ROGÓŻ[1]*, Zbigniew SAWŁOWICZ[1], Paweł SOCHA[2], Krzysztof STEFANIAK[2]

[1] *Institute of Geological Sciences, Jagiellonian University, ul. Oleandry 2a, 30-063 Kraków, Poland; e-mail: anna.rogoz@.uj.edu.pl*

[2] *Institute of Zoology, University of Wrocław, ul. Sienkiewicza 21, 50-335 Wrocław, Poland*

* *Corresponding author*

Received: April 20, 2009
Received in revised form: November 18, 2009
Accepted: November 30, 2009
Available online: December 30, 2009

Abstract. The studied bones and teeth of the cave bear (*Ursus spelaeus)* come from the Biśnik Cave, located in the Częstochowa Upland (Southern Poland). The specimens originate from different geological layers formed since the Odra Glaciation (250–270 thousand years BP). The fossilized bones and teeth were studied using optical microscopy, scanning electron microscopy, X-ray diffraction, FTIR spectroscopy, and INAA. They are built of recrystallized carbonate-rich apatite-(CaOH) and/or apatite-(CaOH). The teeth additionally contain some apatite-(CaF). The lack of collagen and minor REE contents suggest rapid burial and collagen decay in the early stage of diagenesis. The bones and teeth have only limited mineral infillings. In some teeth, Mn-Fe (hydroxy)oxides were found in the dentine canaliculi and in bones, some osteocyte lacunae contain Fe (hydroxy)oxides with admixture of Mn. In one bone specimen, calcite infillings are present in Haversian canals. The infillings formed during later stages of diagenesis and were succeeded by non-filled cracks.

Key-words: bone, teeth, enamel, dentine, apatite, mineral infillings, cave bear

1. Introduction

Though post burial (diagenetic) processes are widely studied today, they are not completely understood and require further research (Pike 1993; Nielsen-Marsh 1997; in Gutiérrez 2001). Diagenetic alterations (chemical and structural, organic and inorganic matter loss) which take place in bones and teeth during diagenesis are a source of information about the taphonomic

history of the bone assemblage (Garland 1987, 1989; Bell 1990; Hedges et al. 1995). Alteration data are also important due to the significance of skeletal remains for dating and stable isotope studies (e.g. Rink, Schwarcz 1995). The isotope- and REE analyses are valuable tools for reconstructing palaeodiet (Kohn et al. 1996; Tütken et al. 2007), metabolism, environmental preferences (Palmqvist et al. 2003) and palaeoclimate (Longinelli 1983; Tütken 2003; Tütken et al. 2004; Tütken et al. 2006). However, the reliability of such data is dependent on knowing the diagenetic history of the skeletal remains (Sillen, Sealy 1995; Brady et al. 2008; Jacques et al. 2008).

The studied specimens come from the Biśnik Cave in the Częstochowa Upland (Southern Poland) where interdisciplinary research has been conducted by archaeologists, zoologists and geologists since 1991. About 100,000 animal remains have been found in the cave sediments. These skeletal remains belong to birds, rodents, carnivores, odd-toed ungulates (Perissodactyla), even-toed ungulates (Artiodactyla) and bats. Among them are extinct animals such as: cave bear (*Ursus spelaeus* Rosenmüller, 1794), cave lion (*Panthera spelaea* Goldfuss, 1810), cave hyena (*Crocuta crocuta spelaea* Goldfuss, 1823), steppe bison (*Bison priscus* Bojanus, 1827), woolly rhino (*Coelodonta antiquitatis* Blumenbach, 1807) and giant deer (*Megaloceros giganteus* Blumenbach, 1897) – as recorded by Wiszniowska et al. (2002).

The aim of this study was to define the degree of their preservation and any diagenetic changes that had occurred. These include decay of organic bone matter, mineral replacement of primary material, infilling of cavities with secondary minerals and changes of crystallinity.

Short bones (metapodia) and (2^{nd} molar) teeth of cave bears were chosen because of their abundance and their presence in different layers in the profile. Bones and teeth were taken from various geological layers. The use of different mineralogical and geochemical methods enabled their chemical and mineralogical characterization.

1.1. General structure of bones and teeth

Bones are built from organic (collagen) and inorganic (apatite-(CaOH)) materials. Bone tissue is a mineralized connective tissue, composed of compact bone (Haversian) and spongy bone (trabecular). The compact bone is the massive, external part of a bone and the spongy bone forms the internal part. The bone is covered with periosteum. The structure of a mammalian compact bone consists of Haversian systems (osteones). Such a system is a bone structural unit which has concentric lamellae (layers of mineralized matrix) deposited around a Haversian canal (central canal). Blood vessels and nerves occur inside those canals. Compact and spongy bones consist of the same material (bioapatite and collagen); the main difference is in the arrangement of the macrostructure (Fig. 1).

Mammalian teeth are sited in alveolar cavities. Tooth is composed of two parts, the crown part above the gum and the root part inside the alveolar cavity. The main part of the tooth is dentine, covered with tooth enamel on the crown and with cementum in the root. The cavity inside the tooth is infilled with pulp. The pulp is a soft tissue and decays easily during diagenesis (Fig. 2).

Teeth and bones are mainly built of bioapatites. Most of the bioapatites are apatite (CaOH) and/or carbonate-rich apatite (CaOH) with Cl^- and F^- ions ($Ca_{10}(PO_4)_6(OH,F,Cl)_2$); there are also bioapatites which do not contain OH^- groups (Wopenka, Pasteris 2005). The enamel,

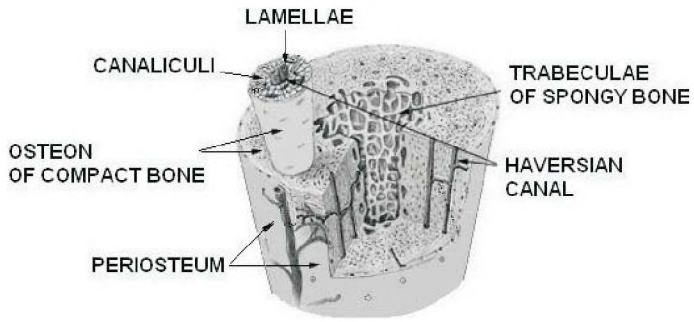

Fig. 1. Schematic structure of a mammalian bone (modified after National Cancer Institute, 2009)

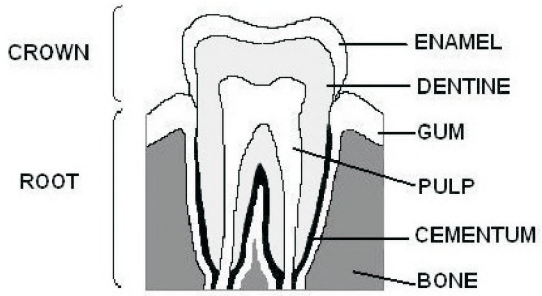

Fig. 2. Schematic structure of a mammalian tooth

the most mineralized part of teeth, contains over 99% apatite by weight (Skinner 2000). The organic matrix of the enamel is not a collagen as in dentine or bone, but comprises amelogenins and enamelins, proteins present only in enamel (Simmer, Fincham 1995; Gross, Berndt 2002). Due to differences in organic matter, enamel bioapatite crystals are larger than those in dentine or bone and are also the part most resistant to chemical and structural changes during diagenesis (Bocherens et al. 1994; Kohn et al. 1999; Elliott 2002; Tütken 2003). Dentine and bones contains 70–72% apatite by weight and 20% organic component (mainly collagen); as they are not as hard as enamel (Elliott 2002), they are more prone to diagenetic change.

2. Geological setting

The Biśnik Cave is located in the Częstochowa Upland in the Niegowonicko-Smoleńskie Hills of the Wodąca Valley in southern Poland (Fig. 3). The valley is filled with Quaternary sediments (Mirosław-Grabowska 1998). On the floor of the valley, red-brown weathered limestone sediments are covered with lake sands and clays, and with aeolian sands on the western slopes (Mirosław-Grabowska 2002). Two entrances of the Biśnik Cave are situated about 5 m above the valley floor (395 m a.s.l.). The thickness of the sediments in the cave is about 7.5 m. An almost continuous sedimentary succession represents the interval since the Odra Glaciation until now (Table 1). There are 20 layers differing in colour, lithology and grain size.

TABLE 1

Stratigraphy and lithology of the sedimentary layers in the Biśnik Cave layers*

	Layer no.	Stratigraphy of the layers	Age in thousands of years	Lithology of the layers	Calcium carbonate contents (%)
Aeolic sediments (III)	1a 1b	Holocene	–	Silty clays	14
	2	Main stadial of the Vistula Glaciation	12–30	Silty clays	6
	3	Grudziądz Interstadial of the Vistula Glaciation	30–50	Beige, medium-grained sands	3.1
	4			Sandy clays, clayey sands	3
Fluvial sediments (II)	5	Gniew Interstadial of the Vistula Glaciation	70–90	Red-yellow, fine-grained sands	0.2
	6 **7**			Fine-grained sands, clayey at the bottom	0.2
Cave sediments (I)	**8**	Torun Stadial of the Vistula Glaciation	90–115	Yellow-brown, sandy silt	3.5
	9			Grey-brown, sandy clays	3
	10			Brown, sandy clays	7
	11			Dark-brown sandy clays	10
	12	Eem Interglacial	115–128	Beige-green sandy clays	1
	13			Yellow-brown, sandy clays	3
	14	Warta Glaciation	128–200	Gray-yellow, dusty loam	6
	15	Lubawa Interglacial	200–250	Yellow-brown, dusty loam	6
	16 17 18 **19**	Odra Glaciation	250–270	Green-brown, dusty loam	6.5–8
	20	Pliocene	–	Residual silt, terra rossa type	–

Data after Mirosław-Grabowska (2002) and Cyrek et al. (2009). Layers that contained the studied specimens are in bold.

The sediments are divided into three sets that differ in their genesis and their way of accumulation. The first set (layers nos. 8–20) accumulated in a cave environment where temperature and humidity conditions were more or less stable. After the accumulation of this set, a part of the cave roof fell in. Due to rising water levels in the Wodąca Valley, a second series of sediments (layers nos. 5–7) was washed into the cave. The third set of sediments (layers nos. 1–4), wind-blown and washed-in, accumulated in the partly open environment (Mirosław-Grabowska 2002). The bones and teeth studied come from all three sediment series (Tables 1, 2). Short

Fig. 3. Location of the Biśnik Cave

TABLE 2

Specimens and methods used

Specimen	Material – methods	CI*	Layer no.
USZ-2	2nd molar tooth: enamel – XRD, INAA dentine – XRD, INAA cementum – XRD, INAA	 0.95 0.12 0.16	2
US-7	short bone (metapodium): compact bone – XRD, INAA spongy bone – XRD, INAA	 0.17	7
USZ-7	2nd molar tooth: enamel – SEM-EDS dentine – SEM-EDS		7
US-8KII	short bone (metapodium): compact bone – XRD, INAA, SEM-EDS spongy bone – XRD, INAA, SEM-EDS	 0.21 0.12	8
USZ-8KII	2nd molar tooth – SEM-EDS		8
US-10	short bone (metapodium): compact bone – XRD, INAA spongy bone – XRD, INAA	 0.13 0.13	10
USZ-11	2nd molar tooth – SEM-EDS		11
USZ-13	2nd molar tooth: enamel – INAA, SEM-EDS dentine – XRD, INAA, SEM-EDS	 0.15	13
US-17p	short bone (metapodium): compact bone – XRD, FTIR, INAA, SEM-EDS spongy bone – XRD, FTIR, INAA, SEM-EDS	 0.13 0.10	19

* CI– crystallinity index of apatite (calculated after Person et al. 1995).

bones, 6–10 cm long, are well preserved (Fig. 4). The teeth have well preserved enamel, cementum and dentine and, in the tooth specimen from layer 19 the alveolar bone is also present. Tooth sizes range from 3–5 cm (Fig. 5).

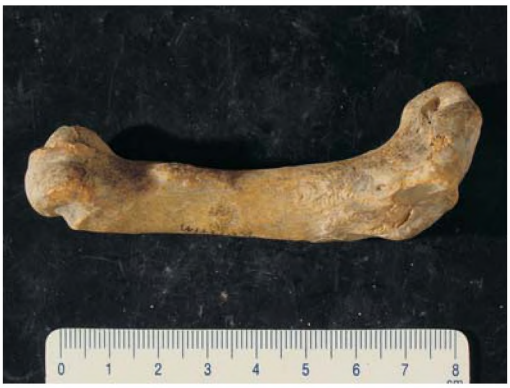

Fig. 4. Cave bear (*Ursus spelaeus*) short (metapodium) bone (USZ11). Scale in cm

Fig. 5. Cave bear (*Ursus spelaeus*) 2nd molar tooth (USZ19). Scale in cm

3. Methods of investigation

Thin sections of the teeth and bones were investigated using a polarising microscope (Nikon Eclipse 6000) and a field emission scanning electron microscope (FE-SEM) HITACHI S-4700 with an energy dispersive spectrometer (EDS) NORAN Vantage analytical system. X-rays diffraction (XRD) analyses were carried out using a Philips-X'Pert APD type diffractometer with a vertical PW 3020 goniometer (Cu Kα radiation monochromatized using a curved graphite crystal monochromator; scan range: 4–60°2Θ). For diffractogram interpretation, the Philips-X'Pert Graphics & Identify program was used. Infrared spectra were obtained with KBr pellets pressed from sample powders using Fourier Transform Infrared Spectrometer (FTIR) BioRad FTS 135 in the wavenumber range 400–4000 cm^{-1}. For trace elements analyses (Instrumental

Neutron Activation Analysis, INAA), a 0.5–2 g sample was weighed into a small custom-made polyethylene vial totally filling it. For every sample, a CANMET WMS-1 standard was co--irradiated with flux wires at a thermal neutron flux of 7×10^{12} n $cm^{-2}s^{-1}$ for 15 minutes in the RIFLS (Reactor Irradiation Facility for Large Samples) site of the McMaster Nuclear Reactor. After 7 days, the samples were counted on a high purity co-axial Ge detector with a resolution of better than 1.7 keV for the 1332 keV ^{60}Co photopeak. Using the flux wire monitors, the data were corrected for decay and compared to a calibration developed from multiple (approx. 50) international reference materials. The CANMET standard WMS-1 was used solely as a check on the procedure and not for calibration purposes. Selected samples were recounted and compared to the originals as part of the QA/QC procedure. Analyses were performed by Activation Laboratories Ltd. (Canada)(Hoffman 1992).

4. Results

4.1. Microscopic observations

In short bones, compact bone and spongy bone are easy to distinguish. Structures such as the Haversian canals or osteocyte lacunae are easily seen. Most of the Haversian canals are not infilled with secondary minerals (Fig. 7). Both the compact and spongy parts of some bones from sandy silt (layer 8) are coated or infilled with calcium carbonate (Fig. 6). Calcium carbonate is also present in pores between the bone trabeculae in spongy parts (Fig. 8, 9). In some of the osteocyte lacunae, iron (hydroxy)oxides (57–79% Fe_2O_3) with some admixture of manganese (0.05–0.64% MnO) occur.

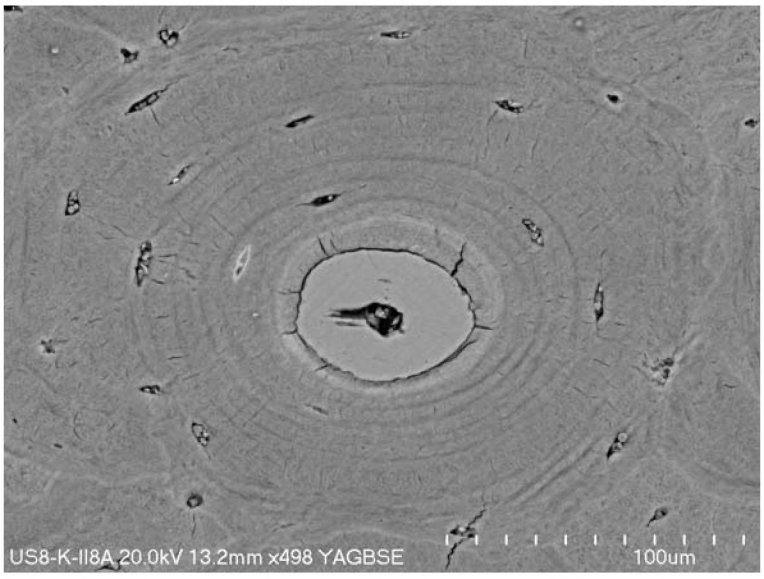

Fig. 6. Haversian canal infilled with calcite and osteocyte lacunae with Fe-Mn (hydroxy)oxides (US8-KII). SEM BSE image

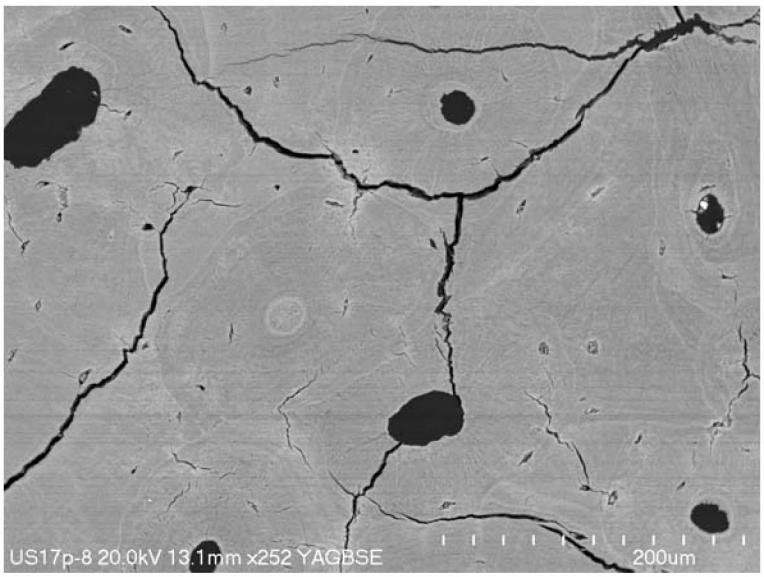

Fig. 7. Compact bone cut by cracks (US17p). SEM BSE image

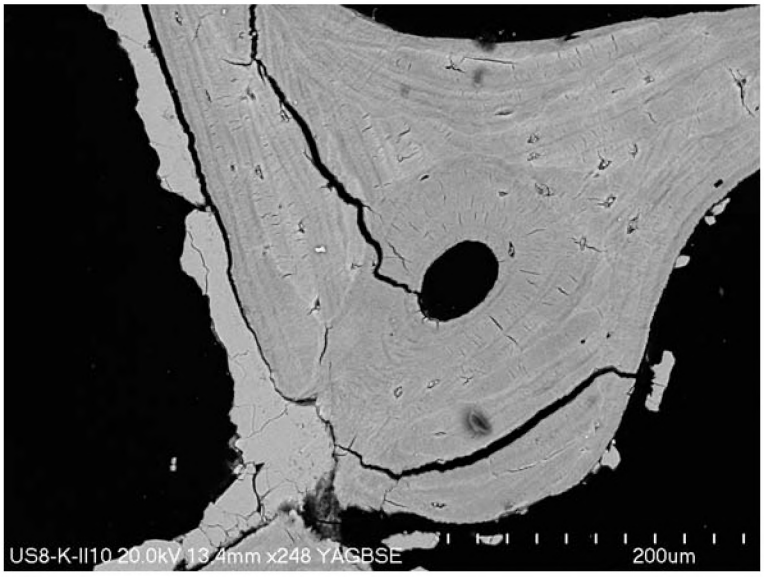

Fig. 8. Calcite around bone trabeculae (US8-KII). SEM BSE image

Though tooth enamel and dentine are both built of apatite, they are easy to distinguish as enamel apatite crystals are bigger and have a more massive structure than those in the dentine. In some teeth, honeycomb or scaley structures that reflect the enamel prisms which are characteristic of tooth enamel are seen (Fig. 10). Canaliculi are observed in the dentine. In backscattered electron image (SEM-BSE), these have light grey rims (Fig. 11, 12) containing

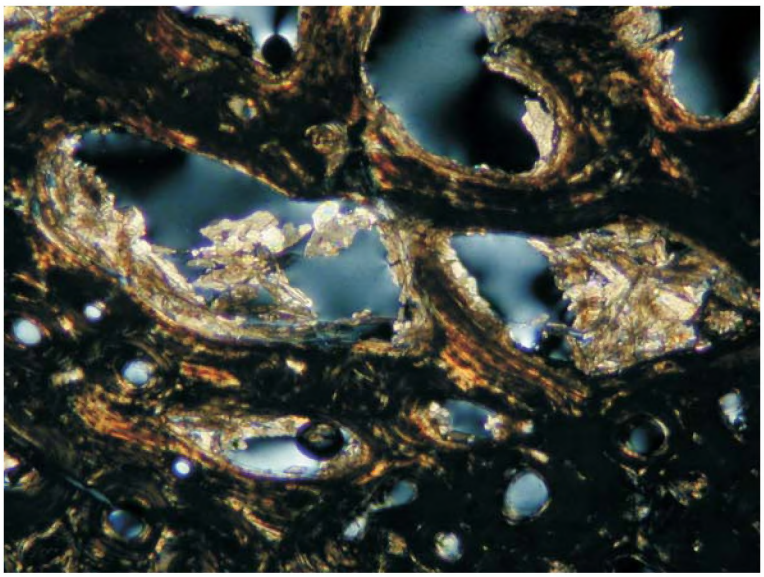

Fig. 9. Calcite between bone trabeculae (US8-KII). Optical microscopy, transmitted light, XP

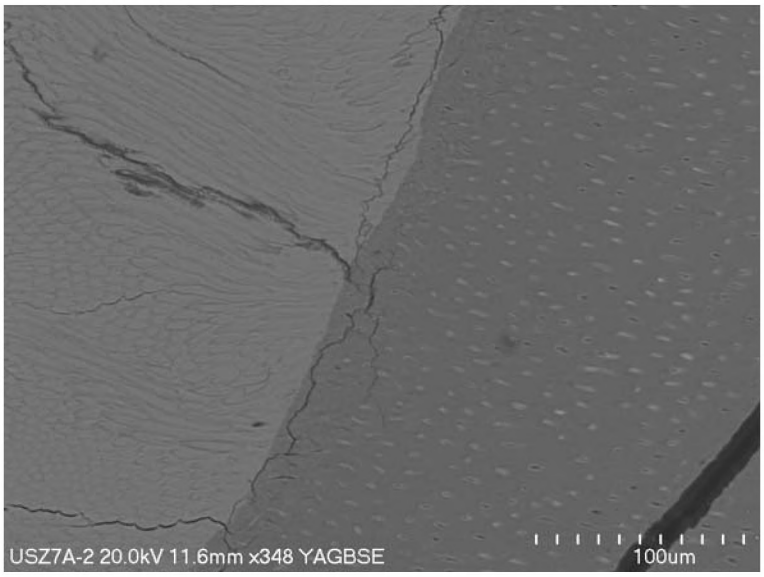

Fig. 10. "Honeycomb" structure in tooth enamel and dentine canaliculi infilled with Mn-Fe(hydroxy)oxides (USZ7A). SEM BSE image

small amounts of Mn and Fe (hydroxy)oxides (0.02–1.15% Fe_2O_3 and 0.01–0.90% MnO). Some are infilled with Mn (hydroxy)oxides (0.35–78% MnO) admixed with Fe (0.15–6% Fe_2O_3). Dentine canaliculi in the tooth from layer 19 are only coated, whereas canaliculi in the teeth from layers nos. 11, 8 and 7 are coated or infilled with Mn and Fe (hydroxy)oxides (Fig. 10, 13).

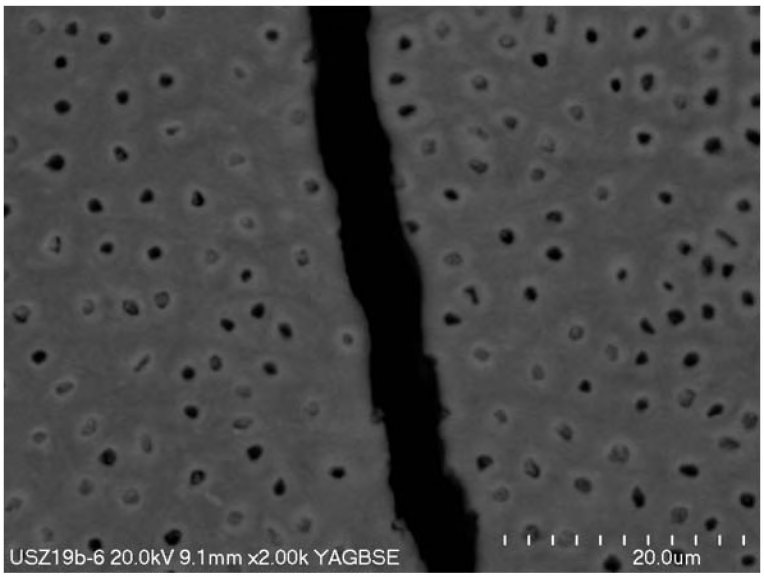

Fig. 11. Dentine canaliculi infilled with Mn-Fe(hydroxy)oxides (USZ19b0). SEM BSE image

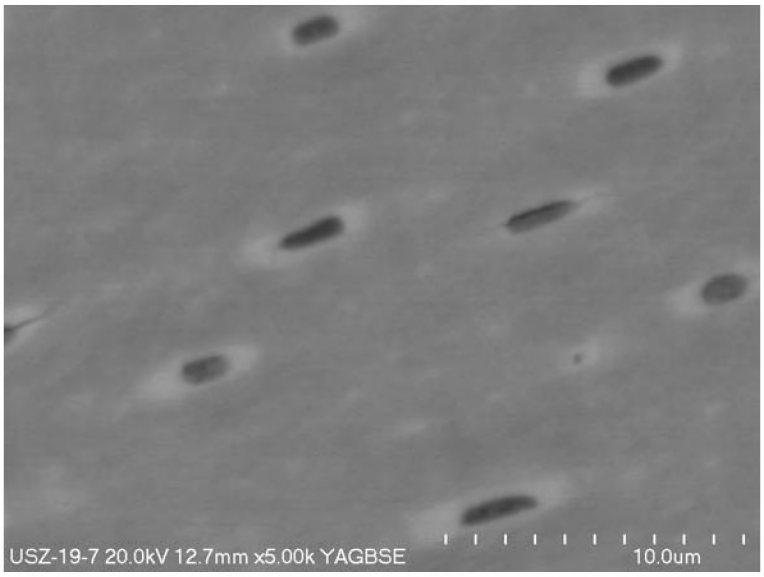

Fig. 12. Dentine canaliculi coated with Mn-Fe (hydroxy)oxides (USZ19b). SEM BSE image

In the canaliculi from layer 11 the infillings are present around the pulp cavity and in those from layers 7 and 8 they are more widely dispersed, even in the parts under the enamel.

The bones and teeth are cut by cracks not infilled with minerals (Fig. 7, 8, 10, 13). Two crack systems are present in the teeth, parallel and perpendicular to the enamel. The parallel cracks occur only in dentine (Fig. 13), in some cases between dentine and enamel. The

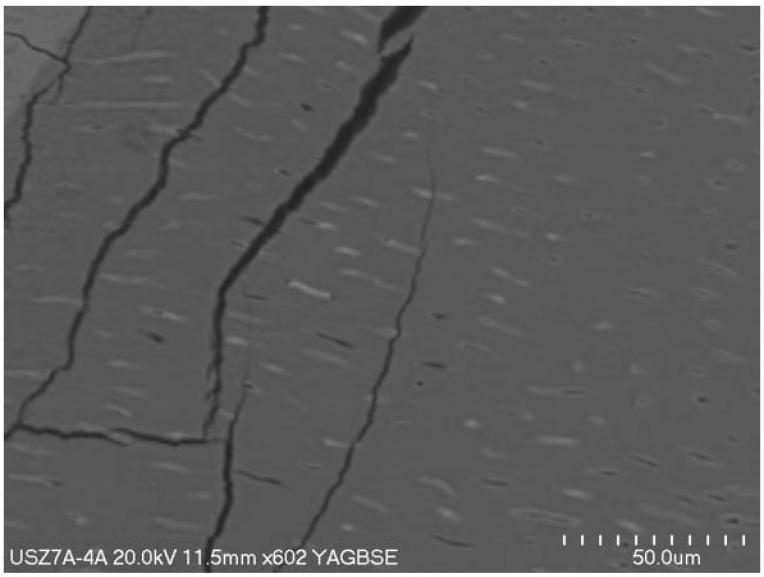

Fig. 13. Dentine canaliculi infilled with Mn-Fe (hydroxy)oxides cut by later cracks (USZ7A). SEM BSE image

perpendicular cracks occur in enamel and dentine; some individual cracks cut both parts. The cracks commonly cut mineral infillings, e.g. in osteocyte lacunae (Fig. 13). The cracks in bones are oriented in many directions. Neither of them exhibit any spatial relationship to histological structures.

4.2. X-ray diffraction and FTIR spectroscopy

The bones and teeth are composed of bioapatite. X-ray patterns do not allow precise distinction between apatite types. All analysed samples, which represent different parts of teeth and bones (spongy bone, compact bone, enamel, dentine and alveolar bone), are built of carbonate rich apatite-(CaOH) and/or apatite-(CaOH) in the case of bones, and additionally of apatite-(CaF) in the case of teeth. In bone samples coming from sandy silt (layer 8) where calcium carbonate infillings were seen using SEM-EDS, calcite is also present (Fig. 14). The calculated crystallinity index values (Table 2; after Person et al. 1995) generally range from 0.10–0.23, independent of material type; the value of 0.95 for enamel of USZ-2 is the exception. The material studied is more crystallized than that of fresh mammalian bones (Fig. 15). Carbonate rich apatite-(CaOH) from enamel is better crystallized than that of dentine, in fact it is best crystallized among all of the samples (Fig. 16). The XRD results are confirmed by FTIR spectroscopy of: compact bone, spongy bone, enamel, dentine and alveolar bone. All infrared spectra are similar. They show phosphate group bands at 471, 564, 603, 1035 cm^{-1} (Elliott 2002), water band at 1652 cm^{-1}, broad water band from 3700–2700 cm^{-1} (Elliott 2002) and carbonate group bands at 872, 1417, 1455, and 1543 cm^{-1} (Fig. 17; Rey et al. 1989; Sønju Clasen, Ruyter 1997; Wychowański et al. 2006).

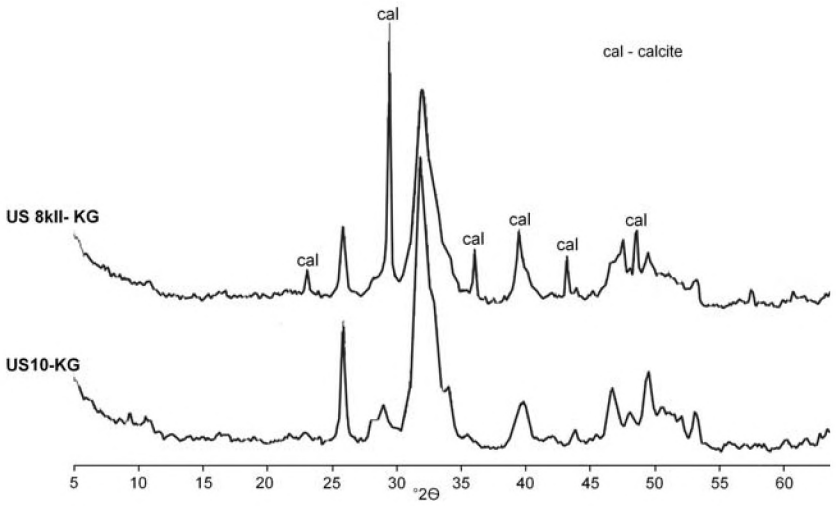

Fig. 14. X-ray pattern of bone apatite-(CaOH) and/or carbonate rich apatite-(CaOH) with calcite infillings (US8-KII) and a typical X-ray pattern of bone apatite-(CaOH) and/or carbonate rich apatite-(CaOH)) without calcite infillings (US 10)

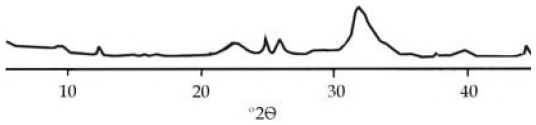

Fig. 15. X- ray pattern of "fresh" bovine bone (peaks represent apatite; after Calafiori et al. 2004)

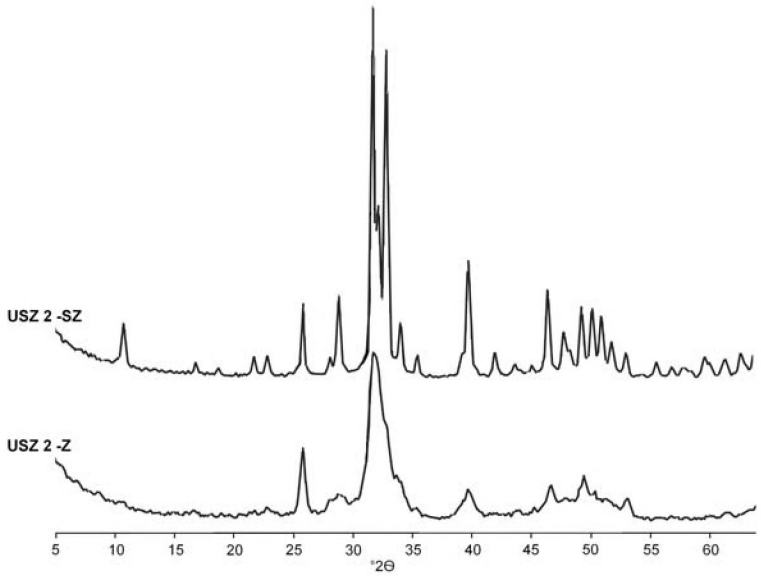

Fig. 16. X-ray pattern of the tooth sample (USZ 2): dentine (USZ 2-Z) and the better crystallized enamel (USZ 2-SZ) (all peaks represent apatite-(CaOH), carbonate rich apatite-(CaOH) and/or apatite-(CaF)

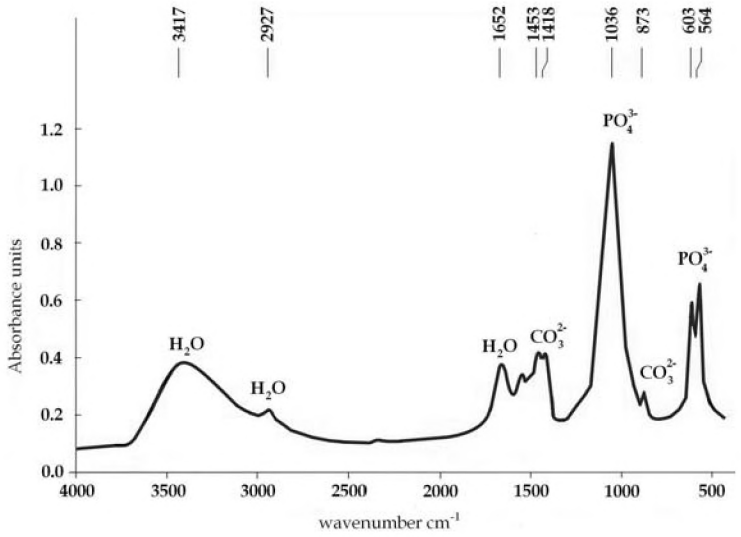

Fig. 17. Infrared spectrum of bone carbonate rich apatite-(CaOH) (US-17 KG)

4.3. Geochemical analyses

Fifteen specimens of different parts of bone and teeth (tooth enamel, dentine, cementum, compact bone and spongy bone) were analysed. The small number of analyses precludes final conclusions but some suggestions may be made. Though contents of the majority of elements are similar in all specimens (Table 3), some reveal specific relationships. In teeth, Ca and Na are higher in enamel than in dentine and cementum. Fe and Zn are lower in enamel than in dentine. Th is higher in cementum than in enamel and dentine. Ba and Br enamel are lower in enamel than in other parts of teeth. Generally, there are no differences in element contents between compact and spongy bone, except that Zn is lower in spongy bone. In the alveolar bone (USZ19b/K), contents of most elements are higher than in the other specimens.

There are some differences in element contents between specimens from various layers. All specimens from layer 2 (USZ 2) are richer in As and Br than those from other layers. Specimens from layer 19 (US 17 and USZ 19b) display highest Cr contents. Ba is lowest in the bone from layer 8 (US 8. Zn in a bone from layer 8 (US 8) and in a tooth from layer 2 (USZ 2) are lower than in other bones and teeth, respectively. Some elements are present in amounts above the detection limit only in single specimens. Au, Ag, Hg, Ir, Mo, Rb, Se, Sn, Sr and Tb are below detection in all specimens.

5. Discussion

In the material studied, the histological structures of teeth and bones are well preserved. No collagen was found, as is common for fossilized bones since collagen typically decays during early diagenesis (Tütken 2003).

TABLE 3

Geochemical analyses (INAA) of the studied specimens

	Element	Au	Ag	As	Ba	Br	Ca	Co	Cr	Cs	Fe	Hf	Hg	Ir	Mo	Na	Ni	Rb	Sb
	Unit Symbol	ppb	ppm	ppm	ppm	ppm	%	ppm	ppm	ppm	%	ppm	ppb	ppm	ppm	%	ppm	ppm	ppm
	Detection Limit	2	5	0.5	50	0.5	1	1	5	1	0.01	1	1	5	1	0.01	20	15	0.1
	Specimen																		
TEETH	USZ2/Z	< 2	< 5	3.3	180	27.7	36	3	< 5	< 1	0.38	< 1	< 1	< 5	< 1	0.31	< 20	< 15	0.4
TEETH	USZ2/C	< 2	< 5	6.4	< 50	40	36	3	8	< 1	0.67	< 1	< 1	< 5	< 1	0.34	< 20	< 15	0.4
TEETH	USZ2/SZ	< 2	< 5	1.2	< 50	6.3	40	1	< 5	< 1	0.18	< 1	< 1	< 5	< 1	0.52	< 20	< 15	< 0.1
TEETH	USZ13/ZC	< 2	< 5	< 0.5	320	6.8	35	4	< 5	< 1	0.13	< 1	< 1	< 5	< 1	0.25	< 20	< 15	0.3
TEETH	USZ13/Z	< 2	< 5	< 0.5	< 50	6.3	32	2	10	< 1	< 0.01	< 1	< 1	< 5	< 1	0.22	140	< 15	0.2
TEETH	USZ19B/Z	< 2	< 5	1,5	110	6.6	34	2	< 5	< 1	0.21	< 1	< 1	< 5	< 1	0.25	< 20	< 15	0.4
TEETH	USZ19B/SZ	< 2	< 5	< 0.5	< 50	4.3	41	2	< 5	< 1	0.11	< 1	< 1	< 5	< 1	0.47	< 20	< 15	< 0.1
TEETH	USZ19B/ZC	< 2	< 5	< 0.5	< 50	8.9	36	4	14	< 1	0.31	< 1	< 1	< 5	< 1	0.24	< 20	< 15	0.4
TEETH	USZ19B/K	< 2	< 5	4	540	11.9	32	5	43	3	1.43	2	< 1	< 5	< 1	0.22	< 20	< 15	0.8
TEETH	USZ19B/C	< 2	< 5	< 0.5	400	8.5	38	1	15	< 1	0.48	< 1	< 1	< 5	< 1	0.31	< 20	< 15	0.6
BONES	US7/KZ	< 2	< 5	< 0.5	310	8.1	32	3	< 5	< 1	0.09	< 1	< 1	< 5	< 1	0.27	< 20	< 15	0.2
BONES	US7/KG	< 2	< 5	< 0.5	200	13.1	33	2	17	< 1	< 0.01	< 1	< 1	< 5	< 1	0.29	< 20	< 15	0.4
BONES	US8KII/KG	< 2	< 5	1.3	< 50	7.6	33	3	< 5	< 1	0.13	< 1	< 1	< 5	< 1	0.28	< 20	< 15	0.3
BONES	US8KII/KZ	< 2	< 5	1.5	80	9	31	1	< 5	< 1	0.1	< 1	< 1	< 5	< 1	0.31	< 20	< 15	0.3
BONES	US10/KZ	< 2	< 5	< 0.5	230	15.8	31	2	< 5	< 1	0.63	< 1	< 1	< 5	< 1	0.26	< 20	< 15	0.4
BONES	US10/KG	< 2	< 5	< 0.5	360	16.6	35	2	13	< 1	0.68	< 1	< 1	< 5	< 1	0.31	< 20	< 15	0.4
BONES	US17/KZ	< 2	< 5	1.6	240	9.7	34	4	16	< 1	0.56	< 1	< 1	< 5	< 1	0.24	< 20	< 15	0.5
BONES	US17/KG	< 2	< 5	0.9	200	11	34	3	29	< 1	0.42	< 1	< 1	< 5	< 1	0.24	90	< 15	0.2

TABLE 3 cont.

	Element	Sc	Se	Sn	Sr	Ta	Th	U	W	Zn	La	Ce	Nd	Sm	Eu	Tb	Yb	Lu	Mass
	Unit Symbol	ppm	ppm	%	%	ppm	ppm	ppm	ppm	ppm	ppm	ppm	ppm	ppm	ppm	ppm	ppm	**ppm**	g
	Detection Limit	0.1	3	0.02	0.05	0.5	0.2	0.5	1	50	0.5	3	5	0.1	0.2	0.5	0.2	0.05	
	Specimen																		
TEETH	USZ2/Z	0.2	< 3	< 0.02	< 0.05	0.7	< 0.2	< 0.5	< 1	170	< 0.5	< 3	< 5	< 0.1	< 0.2	< 0.5	< 0.2	< 0.05	0.205
TEETH	USZ2/C	0.2	< 3	< 0.02	< 0.05	< 0.5	0.5	< 0.5	< 1	110	1	< 3	< 5	< 0.1	< 0.2	< 0.5	0,3	< 0.05	0.200
TEETH	USZ2/SZ	0.2	< 3	< 0.02	< 0.05	< 0.5	< 0.2	< 0.5	< 1	120	1.5	< 3	< 5	< 0.1	< 0.2	< 0.5	< 0.2	< 0.05	0.213
TEETH	USZ13/ZC	0.2	< 3	< 0.02	< 0.05	< 0.5	< 0.2	< 0.5	< 1	530	1.7	< 3	< 5	< 0.1	< 0.2	< 0.5	< 0.2	< 0.05	0.220
TEETH	USZ13/Z	< 0.1	< 3	< 0.02	< 0.05	< 0.5	0.6	< 0.5	< 1	300	1.9	< 3	< 5	< 0.1	< 0.2	< 0.5	< 0.2	< 0.05	0.188
TEETH	USZ19B/Z	0.2	< 3	< 0.02	< 0.05	< 0.5	< 0.2	< 0.5	< 1	500	1.3	< 3	< 5	< 0.1	< 0.2	< 0.5	< 0.2	< 0.05	0.324
TEETH	USZ19B/SZ	0.1	< 3	< 0.02	< 0.05	< 0.5	0.5	< 0.5	< 1	330	1.7	< 3	< 5	< 0.1	< 0.2	< 0.5	< 0.2	< 0.05	0.188
TEETH	USZ19B/ZC	0.3	< 3	< 0.02	< 0.05	< 0.5	0.5	< 0.5	< 1	640	3.2	< 3	< 5	< 0.1	0.3	< 0.5	< 0.2	< 0.05	0.195
TEETH	USZ19B/K	2.7	< 3	< 0.02	< 0.05	0,9	3.8	< 0.5	< 1	2000	16,9	18	23	2.2	0.9	< 0.5	1.4	0.14	0.242
TEETH	USZ19B/C	0.4	< 3	< 0.02	< 0.05	< 0.5	1.8	< 0.5	< 1	1060	5.9	< 3	< 5	0.2	< 0.2	< 0.5	< 0.2	< 0.05	0.180
BONES	US7/KZ	0.2	< 3	< 0.02	< 0.05	< 0.5	1.6	2.5	< 1	710	5.2	< 3	< 5	< 0.1	< 0.2	< 0.5	< 0.2	< 0.05	0.165
BONES	US7/KG	< 0.1	< 3	< 0.02	< 0.05	< 0.5	< 0.2	< 0.5	< 1	230	0.5	< 3	< 5	< 0.1	< 0.2	< 0.5	< 0.2	< 0.05	0.190
BONES	US8KII/KG	0.1	< 3	< 0.02	< 0.05	0.9	0.4	< 0.5	< 1	260	0.9	< 3	< 5	< 0.1	< 0.2	< 0.5	< 0.2	< 0.05	0.218
BONES	US8KII/KZ	0.1	< 3	< 0.02	< 0.05	< 0.5	0.7	< 0.5	< 1	280	0.9	< 3	< 5	< 0.1	< 0.2	< 0.5	< 0.2	< 0.05	0.217
BONES	US10/KZ	< 0.1	< 3	< 0.02	< 0.05	< 0.5	0.4	< 0.5	< 1	510	0.5	< 3	< 5	< 0.1	< 0.2	< 0.5	< 0.2	0.06	0.306
BONES	US10/KG	0.3	< 3	< 0.02	< 0.05	< 0.5	0.8	< 0.5	2	440	0.9	5	< 5	< 0.1	< 0.2	< 0.5	0.2	< 0.05	0.197
BONES	US17/KZ	0.1	< 3	< 0.02	< 0.05	< 0.5	0.5	< 0.5	< 1	660	0.6	< 3	< 5	< 0.1	< 0.2	< 0.5	< 0.2	< 0.05	0.381
BONES	US17/KG	0.2	< 3	< 0.02	< 0.05	< 0.5	< 0.2	< 0.5	< 1	290	0.5	< 3	< 5	< 0.1	< 0.2	< 0.5	< 0.2	< 0.05	0.351

Symbols used after specimen names: SZ – enamel; Z or ZC – dentine; C – cementum; K – alveolar bone; KZ – compact bone; KG – spongy bone.

In some areas tooth enamel retains a very characteristic honeycomb-like structure that is related to the growth of apatite crystals in living teeth. The crystals grow rapidly in width and slowly in thickness and, thus, are flattened hexagons (Elliott 2002). It is also worthy of note that the teeth probably contain apatite-(CaF) in addition to carbonate rich apatite-(CaOH) and/or apatite-(CaOH) found in the bones.

The bones and teeth are both cracked but the directions of cracks vary. In teeth, horizontal cracks occur mainly in enamel. Horizontal and vertical ones are more characteristic of dentine which seems to be related to internal tooth structure. Cracks cut bones and cementum in several directions probably unrelated to histological structure. The cracks probably formed during later diagenesis; they cut earlier Mn-Fe (hydroxy)oxide infillings of tooth canaliculi and calcite infillings of Haversian canals, and none are filled with secondary minerals. According to Pfretzschner (2000), multi-directional cracks form during later diagenesis as the result of external pressure.

Diagenesis significantly influences the mineralogy and geochemistry of teeth and bones. Changes begin during early diagenesis in parts allowing early diffusion, i.e. Haversian canals, osteocyte lacunae in bones and dentine canaliculi, and end during later diagenesis when cracks, sometimes infilled, form (Pfretzschner 2000, 2004). Secondary minerals, the most common being calcite, quartz, pyrite, Fe and Mn oxides, typically fill empty spaces in the fossil bones and teeth (Wings 2004). The studied specimens are relatively poor in secondary minerals, except for small amount of calcite and Mn-Fe (hydroxy)oxides in some. Calcite was found only in Haversian canals and around bone trabeculae and not in osteocyte lacunae, which agrees well with earlier observations by Pfretzschner (2000). The fact that it occurs as infillings only in bones from the sandy silt layer likely reflects the relatively high porosity of that layer.

Relatively rare Fe and Mn (hydroxy)oxides vary in chemical composition mainly between bones and teeth. Fe (hydroxy)oxides, with some Mn admixture, occur in osteocyte lacunae of the bones. The iron may have come from external sources, and/or, as Pfretzschner (2000) hypothesized, from the decay of blood cells during early diagenesis. In the teeth, Mn-Fe (hydroxy)oxides in some of dentine canaliculi are definitely richer in Mn than those in the bones. Kohn et al. (1999) in their study of fresh and fossil mammal teeth from Kenya, found that Mn-Fe (hydroxy)oxides infillings occurred only in the fossils. It seems that forms of the Mn-Fe infillings may relate to the depth of the layer they come from. At the bottom of the section (layer 19), they occur only as coatings of the dentine canaliculi. Higher up (layer 11), infillings occur not only as coatings in the dentine but also occur around pulp cavities. Higher, in layer 7, infillings are present in all dentine, even in the inner part of the tooth under enamel. The mineral coatings and infillings in fossil bone result from solution circulation during diagenesis (Pfretzschner 2004). As the cave was periodically flooded (Mirosław-Grabowska 2002), Fe and Mn rich solutions may have migrated down the section.

In most biological apatites CO_3^{2-} is present. It is released during the metabolism of living organisms (Skinner 2000). The FTIR spectra indicate the substitution of CO_3^{2-} groups (Fig. 17). The carbonate occurs as structural carbonate in the form of A-type substitution for -OH group and B-type substitution for $-PO_4$ group (Rey et al. 1989; Rink, Schwarcz 1995; Sønju Clasen, Ruyter 1997; Fleet, Liu 2004; Sukhodub et al. 2004; Wychowański et al. 2006). The A-type band is 1543 cm^{-1} and the B-type bands are: 872–873 and 1417–1419 cm^{-1}. The 2927 cm^{-1} and 1653 cm^{-1} bands could be amide I bands (Wychowański et al. 2006) but, if so, intense bands

about 1740 cm^{-1} and 3330 cm^{-1} (Wiśniewski et al. 2007) should be present. As they are not, the band probably comes from water molecules (Elliott 2002; Wychowański et al. 2006; Belouafa et al. 2008).

Trace elements contents in fossil bones can vary by several orders of magnitude (Trueman, Tuross 2002; Tütken 2003). Bones and teeth are unstable during diagenesis and elements can be removed or added. Trace metals are adsorbed on the bone surface (Tuross et al. 1989) after death and are introduced into the bone by diffusion during early diagenesis (Trueman, Tuross 2002). In most of the specimens studied, trace-element contents fall among the lower values recorded in the literature.

Some degree of regularity in the distribution of Ca, Na, Zn, Fe, Th, Ba and Br between different tissues of teeth is apparent in the studied samples. Comparison of our data with those in the literature is problematic as few studies involve comparisons between the different tissues of teeth and bones and between living and fossil teeth and bones. For example, higher Ca in enamel is common in living human and animal teeth (Gross, Berndt 2002; Gutiérrez-Salazar, Reyes--Gasga 2003) and higher contents of Na in fossil enamel than in the dentine were also reported by Dauphin and Williams (2004). In our study, we registered higher contents of both Ca and Na in the enamel than in the dentine. Zinc contents usually differ between fresh enamel (c. 1200 ppm; Gross, Berndt 2002) and fresh dentine (c. 700 ppm; Reiche et al. 1999). In our specimens, contents of Zn are usually lower (110–710 ppm) and show no regular enamel-dentine pattern. Trace-element contents vary significantly in bones. Fresh human bones contain < 200 ppm Sr (Trueman, Tuross 2002) whereas, in fossil bones, Sr may vary from < 300 ppm (Hancock et al. 1989) to 9700 ppm (Denys et al. 1996). In our samples, Sr contents are < 500 ppm. Barium, < 10 ppm in fresh human bone (Trueman, Tuross 2002), in fossil bones varies from 268 ppm (Elorza et al. 1999) to 4000 ppm (Denys et al. 1996). In the bones studied by us, Ba contents are generally low (< 50–360 ppm). Zn content in fossil bones is from 90 to 380 ppm (Reiche et al. 1999) and, in the studied bones, Zn is relatively higher (230–710 ppm). The alveolar bone specimen (USZ19b/K) has the highest trace-element contents and is unique in our study; this may reflect either a higher bone porosity or sediment contamination within the pore space.

From the literature, fossil bones clearly show large enrichments in REE over fresh bones (e.g. Hubert et al. 1996; Kohn et al. 1999; Trueman, Tuross 2002). REE contents in fossil bones vary enormously (1–1043 ppm, La – 0.15–142 ppm; Tütken et. al. 2008). Studies of Late Pleistocene fossil bones in the Rhine River gravels suggest that higher REE may reflect greater alteration – a higher degree of collagen decay (Tütken et. al. 2008). In our samples, most REE are below detection limits and La contents are typically low (0.5–0.9 ppm, exceptionally 5.2 ppm). Taphonomy and environmental conditions can significantly promote collagen decay and REE uptake (Tütken et al. 2008 and ref. therein). Rapid burial of the bones and teeth, resulting in fast collagen degradation and increased porosity (Nielsen-Marsh, Hedges 2000), could stimulate rapid apatite recrystallization (Trueman et al. 2004) and a reduced REE uptake from the surroundings.

6. Summary

The cave bear bones and teeth do not contain collagen and apatite is recrystallized. The bones comprise carbonate rich apatite-(CaOH) and/or apatite-(CaOH) and the teeth additionally

contain apatite-(CaF). The lack of collagen, and low REE contents, may indicate rapid burial and collagen decay during early diagenesis. Though most dentine canaliculi, Haversian canals and osteocyte lacunae are not infilled with minerals, locally Fe-Mn (hydroxy)oxides and calcite are present. Mn-Fe infillings are probably related to the depth of source layer. Calcite in Haversian canals and around bone trabeculae occurs only in the material from single sediment layer, therefore probably reflecting its porosity and processes that took place during later diagenesis. Various non-filled cracks cutting the mineral matter of teeth and bones (and pore infillings) developed during late diagenesis as a result of external pressure.

7. References

Bell L.S. (1990). Paleopathology and diagenesis: An SEM evaluation of structural changes using backscattered electron imaging. *Journal of Archaeological Science,* 17, 85–102.

Belouafa S., Chaair H., Loukili H., Digua K., & Sallek B. (2008). Characterization of antiseptic apatite powders prepared at biomimetics temperature and pH. *Materials Research,* 11(1), 93–96. DOI: 10.1590/S1516-14392008000100018

Bocherens H., Brinkam D.B., Dauphin Y., & Mariotti A. (1994). Microstructural and geochemical investigations on late Cretaceous archosaur teeth from Alberta, Canada. *Canadian Journal of Earth Science,* 31, 783–792.

Brady A.C., White C.D., Longstaffe F.J., & Southham G. (2008). Investigating intra-bone isotopic variations in bioapatite using IR- laser ablation and micromilling: Implications for identifying diagenesis? *Palaeogeography, Palaeoclimatology, Palaeoecology,* 266, 190–199. DOI: 10.1016/j.palaeo.2008.03.031.

Calafiori A.R., Marotta M., Nastro A., & Martino G. (2004). Low temperature method for the production of calcium phosphate fillers. *BioMedical Engineering Online,* 3, 8. DOI: 10.1186/1475-925X-3-8.

Cyrek K., Mirosław-Grabowska J., Stefaniak K., & Socha P. (2009). Archaeology, stratigraphy and palaeoecology of the Biśnik Cave. In K. Stefaniak, P. Socha & A. Tyc (Eds.), *Karst of the Częstochowa Upland and the Eastern Sudetes – Palaeoenvironments and Protection* (pp. 77–98). Sosnowiec–Wrocław, Poland: Top Art.

Dauphin Y., & Williams C.T. (2004). Diagenetic trends of dental tissues. *Comptes Rendus Palevol,* 3(6–7), 583–590. DOI: 10.1016/j.crpv.2004.07.007.

Denys C., Wiliam C.T., Dauphin Y., Andrews P., & Fernandez-Jalvo Y. (1996). Diagenetical changes in Pleistocene small mammals bones from Olduvai Bed-1. *Palaeogeography, Palaeoclimatology, Palaeoecology,* 126, 121–134.

Elliott J.C. (2002). Calcium phosphate biominerals. *Reviews in Mineralogy and Geochemistry,* 48, 427–453. DOI: 10.2138/rmg.2002.48.11.

Elorza J., Astibia H., Murelaga X., & Pereda-Suberbiola X. (1999). Francolite as a diagenetic mineral in dinosaur and other Upper Cretaceous reptile bones (Laño, Iberian Peninsula): microstructural, petrological and geochemical features. *Cretaceous Research,* 20, 169–187. DOI: 10.1006/cres.1999.0144.

Fleet M.E., & Liu X. (2004). Location of type B carbonate ion in type A–B carbonate apatite synthesized at high pressure. *Journal of Solid State Chemistry, 177,* 3174–3182. DOI: 10.1016/j.jssc.2004.04.002.

Garland A.N. (1987). Palaeohistology. *Science and Archaecology,* 29, 25–29.

Garland A.N. (1989). Microscopical analysis of fossil bone. *Applied Geochemistry,* 4, 215–229.

Gross K.A. & Berndt C.C. (2002). Biomedical Application of Apatites. *Reviews in Mineralogy and Geochemistry,* 48, 631–673. DOI: 10.2138/rmg.2002.48.17

Gutiérrez M. (2001). Bone diagenesis and taphonomic history of the Paso Otero 1 bone bed, Pampas of Argentina. *Journal of Archaeological Science,* 28, 1277–1290. DOI: 10.1006/jasc.2000.0648

Gutiérrez-Salazar M., & Reyes-Gasga J. (2003). Microhardness and chemical composition of human tooth. *Material Research,* 6, 1–7. DOI: 10.1590/S1516-14392003000300011

Hancock R.G.V., Grynpas M.D., & Pritzker K.P.H. (1989). The abuse of bone analyses for archeological dietary studies. *Archaeometry,* 31, 169–179.

Hedges R.E.M., Millard A.R., & Pike A.W.G. (1995). Measurements and relationships of diagenetic alteration of bone from three archaeological sites. *Journal of Archaeological Science,* 22, 201–209.

Hoffman E.L. (1992). Instrumental neutron activation in geoanalysis. *Journal of Geochemical Exploration,* 44, 297–319.

Hubert J.F., Panish P.T., Chure D.J., & Prostak K.S. (1996). Chemistry, microstructure, petrology, and diagenetic model of Jurassic dinosaur bones, Dinosaur National Monument, Utah. *Journal of Sedimentary Research,* 66, 531–547.

Jacques L., Ogle N., Moussa I., Kalin R., Vignaud P., Brunet M., & Bocherens H. (2008). Implications of diagenesis for the isotopic analysis of Upper Miocene large mammalian herbivore tooth enamel from Chad. *Palaeogeography, Palaeoclimatology, Palaeoecology,* 266, 200–210. DOI: 10.1016/j.palaeo.2008.03.040.

Kohn M.J., Schoeninger M.J., & Valley J.W. (1996). Herbivore tooth oxygen compositions: Effects on diet and physiology. *Geochimica et Cosmochimica Acta,* 60, 3889–3896. DOI: 10.1016/0016-7037(96)00248-7.

Kohn M.J., Schoeninger J., & Barker W.W. (1999). Altered states: Effect on fossil tooth chemistry. *Geochimica et Cosmochimica Acta, 63,* 2737–2747. DOI: 10.1016/S0016-7037(99)00208-2.

Longinelli A. (1983). Oxygen isotopes in mammal bone phosphate: a new tool for paleohydrological and paleoclimatological research? *Geochimica et Cosmochimica Acta,* 48, 385–390.

Mirosław-Grabowska J. (1998). Stratygrafia osadów czwartorzędowych wschodniej części Pasma Smoleńsko-Niegowonickiego (Wyżyna Krakowsko-Częstochowska). *Studia Geologica Polonica,* 113, 105–119.

Mirosław-Grabowska J. (2002). Litologia i stratygrafia osadów Jaskini Biśnik. In K. Cyrek (Ed.), *Jaskinia Biśnik. Rekonstrukcja zasiedlenia jaskini na tle zmian środowiska przyrodniczego* (pp. 143–179). Toruń, Poland: Wydawnictwo Uniwersytetu Mikołaja Kopernika.

National Cancer Institute (2009). Compact Bone and Spongy (Cancellous Bone). Retriéed November 6, 2009, from http://training.seer.cancer.gov/images/anatomy/skeletal/bone_tissue.jpg

Nielsen-Marsh C. M. (1997). *Studies in Archaeological Bone Diagenesis*. Unpublished doctoral thesis, University of Oxford, United Kingdom.

Nielsen-Marsh C.M., & Hedges R.E.M. (2000). Patterns of diagenesis in bones I: The effects of site environments. *Journal of Archaeological Science,* 27, 1139–1150. DOI: 10.1006/jasc.1999.0537.

Palmqvist P., Gröcke D.R., Arribas A., & Fariña R.A. (2003). Paleoecological reconstruction of a lower Pleistocene large mammal community using biogeochemical ($\delta^{13}C$, $\delta^{15}N$, $\delta^{18}O$, Sr:Zn) and ecomorphological approaches. *Paleobiology,* 29, 205–229. DOI: 10.1666/0094-8373(2003)029<0205:PROALP>2.0.CO;2.

Person A., Bocherens H., Saliege J.F., Paris F., Zeitoun V., & Gerard M. (1995). Early diagenetic evolution of bone phosphate: an X-ray diffractometry analysis. *Journal of Archaeological Science* 22, 211–221.

Pike A.W.G. (1993). *Bone Porosity, Water and Diagenesis: Towards a Grand Unified Theory of Bone Diagenesis.* Unpublished Bachelor Thesis. University of Bradford, United Kingdom.

Pfretzschner H.U. (2000). Microcracks and fossilization of Haversian bone. *Neue Jahrbuch für Geologie und Paläontologie Abhandlungen,* 216, 413–431.

Pfretzschner H.U. (2004). Journal of Archaeological Science: Fossilization of Haversian bone in aquatic environments. *Comptes Rendus Palevol,* 3, 605–616. DOI: 10.1016/j.crpv.2004.07.006.

Reiche I., Favre-Quattropani L., Calligaro T., Salomon J., Bocherens H., Charlet L., & Menu M. (1999). Trace element composition or archaeological bones and postmortem alteration in the burial environment. *Nuclear Instruments and Methods in Physics Research,* 150, 656–662. DOI: 10.1016/S0168-583X(98)00949-5.

Rey C., Collins B., Goehl T., Dickson R., & Glimsher M.J. (1989). The carbonate environment in bone mineral: A resolution-enhanced Fourier transform infrared spectroscopy study. *Calcified Tissue International,* 45, 157–164.

Rink W.J., & Schwarcz H.P. (1995). Tests for diagenesis in tooth enamel: ESR dating signals and carbonate contents. *Journal of Archaeological Science,* 22, 251–255.

Sillen A., & Sealy J.C. (1995). Diagenesis of strontium in fossil bone: A reconsideration of Nelson et al. (1986). *Journal of Archaeological Science,* 22, 313–320. DOI: 10.1006/jasc.1995.0033.

Simmer J.P., & Fincham A.G. (1995). Molecular mechanism of dental enamel formation. *Critical Reviews in Oral Biology & Medicine,* 6, 84–108. DOI: 10.1177/10454411950060020701.

Skinner H.C.W. (2000). In praise of phosphates, or why vertebrates chose apatite to mineralize their skeletons. *International Geological Review,* 42, 232–240.

Sønju Clasen A.B, & Ruyter I.E. (1997). Quantitative determination of type A and type B carbonate in human deciduous and permanent enamel by means of Fourier Transform Infrared Spectrometry. *Advances in Dental Research,* 11, 523–527. DOI: 10.1177/08959374970110042101.

Sukhodub L.F., Moseke C., Sukhodub L.B., Sulkio-Cleff B., Maleev V.Ya., Semenov M.A., Bereznyak E.G., & Bolbukh T.V. (2004). Collagen-hydroxyapatite-water interactions investigated by XRD, piezogravimetry, infrared and Raman spectroscopy. *Journal of Molecular Structure,* 704, 53–58. DOI: 10.1016/j.molstruc.2003.12.061.

Trueman C.N., & Tuross N. (2002). Trace elements in recent and fossil bone apatite. *Reviews in Mineralogy and Geochemistry,* 48, 489–521. DOI: 10.2138/rmg.2002.48.13.

Trueman C.N., Behrendsmeyer A.K., Tuross N., & Weiner S. (2004). Mineralogical and compositional changes in bones exposed on soil surfaces in Amboseli National Park, Kenya: diagenetic mechanism and the role of sediment pore fluids. *Journal of Archaeological Science,* 31, 721–739. DOI: 10.1016/j.jas.2003.11.003.

Tuross N., Behrensmeyer A.K., & Eanes E.D. (1989). Strontium increases and crystallinity changes in taphonomic and archaeological bone. *Journal of Archaeological Science,* 16, 661–672.

Tütken T. (2003). *Die Bedeutung der Knochenfrühdiagenese für die Erhaltungsfähigkeit in vivo erworbener Element- und Isotopenzusammensetzungen in fossilen Knochen.* Unpublished doctoral dissertation, University of Tübingen, Germany.

Tütken T., Pfretzschner H.U., Vennemann T.W., Sun G., & Wang Y.D. (2004). Palaeobiology and skeletochronology of Jurassic dinosaurs: implications from the histology and oxygen isotope compositions of bones. *Palaeogeography, Palaeoclimatology, Palaeoecology,* 206, 217–238. DOI: 10.1016/j.palaeo.2004.01.005.

Tütken T., Vennemann T.W., Janz H., & Heizmann E.P.J. (2006). Palaeoenvironment and palaeoclimate of the Middle Miocene lake in the Steinheim basin, SW Germany: A reconstruction from C, O, and Sr isotopes of fossil remains. *Palaeogeography, Palaeoclimatology, Palaeoecology,* 241, 457–491. DOI: 10.1016/j.palaeo.2006.04.007.

Tütken T., Furrer H., & Vennemann T.W. (2007). Stable isotope compositions of mammoth teeth from Niederweningen, Switzerland: Implications for the Late Pleistocene climate, environment and diet. *Quaternary International,* 164–165, 139–150. DOI: 10.1016/j.quaint.2006.09.004.

Tütken T., Vennemann T.W., & Pfretzschner H.U. (2008). Early diagenesis of bone and tooth apatite in fluvial and marine settings: Constraints from combined oxygen isotope, nitrogen and REE analysis. *Palaeogeography, Palaeoclimatology, Palaeoecology,* 266, 254–268. DOI: 10.1016/j.palaeo.2008.03.037.

Wings O. (2004). Authigenic minerals in fossil bones from the Mesozoic of England: poor correlation with depositional environments. *Palaeogeography, Palaeoclimatology, Palaeoecology,* 204, 15–32. DOI: 10.1016/S0031-0182(03)00709-0.

Wiszniowska,T., Socha, P., & Stefaniak, K. (2002). Czwartorzędowa fauna z osadów Jaskini Biśnik. In K. Cyrek (Ed.), *Jaskinia Biśnik. Rekonstrukcja zasiedlenia jaskini na tle zmian środowiska przyrodniczego*, 192–220. Toruń, Poland: Wydawnictwo Uniwersytetu Mikołaja Kopernika.

Wiśniewski M., Sionkowska A., Kaczmarek H., Lazare S., & Tokarev V. (2007). Wpływ promieniowania laserowego na cienkie błony kolagenowe (Influence of laser irradiation on the thin collagen films). *Polimery,* 52, 571–578.

Wopenka B., & Pasteris J.D. (2005). A mineralogical perspective on the apatite in bone. *Materials Science and Engineering: C.*, 25, 131–143. DOI: 10.1016/j.msec.2005.01.008.

Wychowański P., Kolmas L., Kalinowski E., Krzywicki D., Chomicki P., Gąsiorowska M., Wojtowicz A., & Kołodziejski W. (2006). Analiza porównawcza szkliwa i zębiny ludzkich zębów prawidłowych i nadliczbowych metodą mikrospetroskopii w zakresie średniej podczerwieni. *Dental and medical problems,* 43, 53–57.